U. S. DEPARTMENT OF COMMERCE
NATIONAL OCEANIC AND ATMOSPHERIC ADMINISTRATION
NATIONAL WEATHER SERVICE
NATIONAL METEOROLOGICAL CENTER

OFFICE NOTE 141

Global Data Assimilation by Local Optimum Interpolation

R. D. McPherson, K. H. Bergman
R. E. Kistler, G. E. Rasch, and D. S. Gordon
Development Division

MARCH 1977

Presented at the AMS Third Conference on Numerical Weather Prediction,
Omaha, Nebraska, April 26-28, 1977.

Global Data Assimilation by Local Optimum Interpolation

I. Introduction

Over the past decade, the planners of the First GARP Global Experiment (FGGE) have labored to assure that the meteorological observing system extant during the Experiment would provide truly global coverage on a nearly continuous basis. The mix of subsystems now planned includes geostationary and polar-orbiting satellites, buoys, constant-level balloons, and specially-instrumented commercial aircraft, in addition to the conventional radiosonde and surface-observing network. Data from these varied sources will exhibit widely varying characteristics with respect to parameters observed, distribution in space and time, and error levels. A flexible data assimilation system capable of intelligently blending these disparate observations into a complete and consistent numerical representation of the atmosphere is necessary.

A system incorporating the required flexibility is being constructed at the National Meteorological Center (NMC). Development has progressed to a point where initial tests have been completed, some results of which are reported in this paper. A description of the system is presented in the next section, followed by a discussion of the results of the initial testing. The final section outlines our plans for future work with the system.

II. Description of the Assimilation System

The assimilation system requires the availability of a sophisticated, high-resolution prediction model capable of very accurate short-term forecasts. It is assumed that the prediction, at any given time, represents

the atmosphere with a reasonably high degree of fidelity. From this assumption, it follows that

- relatively small adjustments are required to correct the model atmosphere; and
- in the absence of observations, no arbitrary or incidental adjustments need be made.

These two statements form the basis of the system's design.

At any time, the model representation may be corrected by the availability of timely observations. This is done by a process of local updating; i.e., local in the sense of affecting only those grid points within a specified neighborhood of the observations. Updating is performed by three-dimensional interpolation of forecast residuals (differences between observed temperature, wind, and specific humidity, and their predicted counterparts interpolated to the observation locations) to the model grid points. The interpolation is quasi-statistical, based on the "optimum interpolation" procedures of Gandin (1963). Differing error characteristics of different observing systems are explicitly incorporated. The system is very similar in design to one presently in operational use at the Canadian Meteorological Centre (Rutherford, 1976) and to that developed by Schlatter (1976) at the National Center for Atmospheric Research.

A brief summary of the interpolation procedure follows. For a detailed account, the reader is referred to Bergman (1977). Let the observed temperature and wind components (T, U, V) be composed of a

"guess" value ($\overline{T}$, $\overline{U}$, $\overline{V}$) plus a deviation (t, u, v). Then the updated temperature and winds at a grid point (T_g, U_g, V_g) may be expressed as linear combinations of the deviational quantities,

$$\begin{aligned} T_g &= \overline{T}_g + \sum_{i=1}^{\ell} a_i t_i + \sum_{j=1}^{m} b_j u_j + \sum_{k=1}^{n} c_k v_k \\ U_g &= \overline{U}_g + \sum_{i=1}^{\ell} a_i' t_i + \sum_{j=1}^{m} b_j' u_j + \sum_{k=1}^{n} c_k' v_k \\ V_g &= \overline{V}_g + \sum_{i=1}^{\ell} a_i'' t_i + \sum_{j=1}^{m} b_j'' u_j + \sum_{k=1}^{n} c_k'' v_k \end{aligned} \tag{1}$$

where there are ℓ temperature deviations, m west wind deviations, and n south wind deviations. The quantities ($\overline{T}_g$, $\overline{U}_g$, $\overline{V}_g$) are the "guess" values at the gridpoint. The unknown coefficients a, b, c, etc., may be determined by requiring minimization of the mean-square interpolation error,

$$E = \overline{(T_g - \overline{T}_g - \sum_{i=1}^{\ell} a_i t_i - \sum_{j=1}^{m} b_j u_j - \sum_{k=1}^{n} c_k v_k)^2} \tag{2}$$

where the overbar denotes an ensemble average. This leads to a system of linear equations

$$\begin{aligned} &\sum_{i=1}^{\ell} \overline{t_{\ell'} t_i} a_i + \sum_{j=1}^{m} \overline{t_{\ell'} u_j} b_j + \sum_{k=1}^{n} \overline{t_{\ell'} v_k} c_k = \overline{t_{\ell'} t_g}, \quad \ell' = 1,\ell \\ &\sum_{i=1}^{\ell} \overline{u_{m'} t_i} a_i + \sum_{j=1}^{m} \overline{u_{m'} u_j} b_j + \sum_{k=1}^{n} \overline{u_{m'} v_k} c_k = \overline{u_{m'} t_g}, \quad m' = 1,m \\ &\sum_{i=1}^{\ell} \overline{v_{n'} t_i} a_i + \sum_{j=1}^{m} \overline{v_{n'} u_j} b_j + \sum_{k=1}^{n} \overline{v_{n'} v_k} c_k = \overline{v_{n'} t_g}, \quad n' = 1,n \end{aligned} \tag{3}$$

and similar systems for U_g and V_g. If the autocorrelations ($\overline{t_\ell t_i}$, $\overline{u_m u_j}$, $\overline{v_n v_k}$) and the cross-correlations ($\overline{t_\ell u_j}$, etc.), as well as the correlations between the observed and interpolated deviations, are known, then the system can be solved for the coefficients a_i, b_j, c_k. According to Gandin, if the correlations are obtained from actual data, then the interpolation is statistically "optimal " in the sense of minimization of eqn. (2). In practice, however, it is much more convenient to model the autocorrelations with differentiable, analytic functions, and then obtain the cross-correlations by means of the thermal wind equation. The more pragmatic approach was adopted here.

Observational errors are accounted for in the following way: For any of the auto-correlation functions, the actual value of the deviational quantity $\hat{f}$ is composed of the true value of f plus an error ε. The correlation is then

$$\overline{\hat{f}_i \hat{f}_j} = \overline{(f_i+\varepsilon_i)(f_j+\varepsilon_j)} = \overline{f_i f_j} + \overline{f_i \varepsilon_j} + \overline{f_j \varepsilon_i} + \overline{\varepsilon_i \varepsilon_j} \qquad (4)$$

For most conventional observations, errors are assumed random: Thus,

$$\begin{aligned} \overline{\hat{f}_i^2} &= \overline{f_i^2} + \overline{\varepsilon_i^2}, \quad i = j \\ \overline{\hat{f}_i \hat{f}_j} &= \overline{f_i f_j}, \qquad i \neq j, \end{aligned} \qquad (5)$$

and $\overline{\varepsilon_i^2}$ may be specified for each type of observation. For some types of remote-sounding data, however, the errors may be correlated with each other, so that

$$\overline{\hat{f}_i \hat{f}_j} = \overline{f_i f_j} + \overline{\varepsilon_i \varepsilon_j}, \qquad (6)$$

and the error correlation must be specified. It has customarily been assumed that the second and third terms of eqn. (4) vanish; that is, the errors are uncorrelated with the true field. It may be, however, that some types of remote sounding data tend to underestimate the amplitudes of meteorological systems. Thus, observations would tend to underestimate heights in ridges and overestimate them in troughs. If so, the errors and the true field would be correlated and account would have to be taken of the two neglected terms. The error terms in (5) and (6) enter the system through augmentation of the elements of eqns. (3), and must be prespecified.

The system of eqns. (3), together with their counterparts for U_g and V_g, constitute three systems of $(\ell + m + n)$ equations to be solved for each gridpoint to be updated. The manner in which this is done is discussed in a subsequent section.

The prediction model that provides the forecasts is the NMC global primitive equation model (Stackpole, et al., 1974). The gridpoints to be updated are therefore intersections of parallels and meridians in the horizontal, and the midpoints of the layers in the vertical. In the present application, the horizontal resolution is 5 degrees, the update interval is 6 hours, and there are eight layers in the vertical. Figure 1 shows the vertical structure of the model.

Figure 2 outlines the significant events occurring at each update. Since the updating is performed in the model's coordinates, and its vertical

coordinate is time-varying, the vertical coordinate itself must be updated as the first step. This is done in three stages: an update of the model surface pressure P_*; an update of the model "tropopause" pressure P_{**}; and a redefinition of the pressures at the midpoints of the layers and interpolation of the forecast variables to the redefined midpoints.

A. Updating the vertical coordinate

1. Surface pressure update

The prediction model produces a forecast of the pressure at the elevations of the model gridpoints. The dominant variation of this field is due to terrain. In order to separate this variation from that due to meteorological systems, the standard atmosphere pressure at the terrain elevation of each gridpoint is subtracted from the predicted surface pressure. The resulting field of departure from standard atmosphere (D-values of surface pressure) is the field to be updated.

The data are station pressure observations, if available; if not reported, mean-sea-level observations are accepted only if the station elevation is less than 500 m. Conversion to D-values is done by subtracting the standard atmosphere pressure at the station elevation from the reported station pressure. A hydrostatic adjustment is performed to allow for the difference between the actual elevation of the reporting station and smoothed model elevation. The adjusted observations are then subjected to a gross error check; those not rejected are passed to the interpolation routine.

The updating procedure uses the optimum interpolation outlined previously. Residuals of both station pressure and wind are calculated, but wind residuals are permitted to influence only marine and coastal gridpoints. The winds are corrected for frictional effects through the empirical formulae of Cardone (1969).

The updated field of surface pressure departures is then recombined with the standard atmosphere pressure at the model terrain. The resulting field is then used in the redefinition of the vertical coordinate.

2. "Tropopause" update

The material surface which separates the model's lower six layers from the upper layers is intended to approximate the location of the actual tropopause at the beginning of the forecast. However, there is no attempt to model atmospheric behavior near the tropopause, so that during the course of an extended forecast the material surface does not necessarily retain close resemblance to the actual tropopause. Occasionally, this lack of similarity degenerates into serious numerical problems capable of terminating the prediction. For these reasons, it is necessary to update the material surface in such a way that the corrections are small and the updated surface well behaved.

To insure that the updating process does not perpetuate numerical difficulties around the material surface, a climatological tropopause, varying only with latitude, is blended with the predicted

pressure at the material surface. This blended field is then used as the "guess" to be corrected by data through optimum interpolation. Observations of tropopause pressure as reported by radiosondes are used directly. Values of tropopause pressure are calculated for radiometric soundings by calculating a least-squares fit of the mandatory-level temperatures to a fifth-order polynomial and then locating the minimum of the polynomial.

Differences are then formed between the observations and the blended forecast/climatological field interpolated bilinearly to the locations of the observations. These differences are then used to update the blended field at the gridpoints through univariate optimum interpolation. The capability to filter the correction fields before recombining with the blended guess field exists, although it need not be utilized.

3. Adjustment of predicted fields

The updated fields of the surface pressure and tropopause pressure are then used to redefine the vertical coordinate according to the formula

$$\sigma_T = \frac{P - P_{**}}{P_* - P_{**}} \quad , \quad P > P_{**}$$

and (7)

$$\sigma_s = \frac{P - 50}{P_{**} - 50} \quad , \quad 50 < P < P_{**}$$

Small changes ($\simeq$ 10 mb) in P_* and P_{**} therefore result in even smaller changes in the pressures at the midpoints of the layers. The predicted

values of T, u, v, and q at the midpoints of the "old" layers are adjusted to the updated levels by an interpolation which is linear in the logarithm of pressure. No interpolation is permitted across the model tropopause.

This step completes the first part of the update cycle; the next step is the updating of the winds and temperature multivariately; and moisture, univariately.

B. Updating the history variables

1. Data preparation

The upper air data base, containing observations of temperature, wind, and dewpoint depression, must be ordered by latitude and longitude. Each temperature, wind, and dewpoint depression observation, together with its position (latitude, longitude, and pressure) and instrument type, is stratified according to longitude within 2.5 degree latitude bands. These data are then passed to a routine which interpolates (bilinearly) the corresponding forecast parameter to the locations of the data, and differences are calculated. Dewpoint depression is converted to specific humidity, since the latter is the moisture history variable in the prediction model.

At this point, the residuals are subjected to a two-stage error check.* Each individual residual is compared to the mean and standard deviation for its latitude band. The means and standard

---

*It should be noted that several error checks are incorporated in the operational decoding and processing of the raw data.

deviations are presently prespecified, but ultimately will be recalculated for each update. Unconditional acceptance occurs if the residual is within $N_1\sigma$ of the mean, and unconditional rejection if outside $N_2\sigma$, where N_1 and N_2 are determined by experience. For residuals in the marginal area between $N_1\sigma$ and $N_2\sigma$, further checking is necessary. It is intended to eventually subject these marginal observations to a "buddy check"; that is, to determine if a questionable datum is supported by near neighbors. At the moment, however, the marginal observations are merely flagged, but accepted.

Each accepted observation is then assigned an error level according to the instrument type. Table 1 presents the values currently in use; these are in many cases quite arbitrary, and in all cases subject to revision as additional information becomes available.

2. Data selection

In principle, the number of observations that influence each update should be all those which are significantly correlated with the updated gridpoint. However, the number actually used ($\ell + m + n$ in eqns. 3) determines the dimensions of the system of equations to be solved. Computational limitations therefore require a compromise with principle. The present version allows a maximum of ten observations to influence each update. The selection of the ten observations is an intricate procedure, based generally on locating those observations which give maximum values to the right-hand-sides of eqns. (3). For details of the selection process, the reader is again referred to Bergman (1977).

3. Solution of the linear system

Once the ten (or fewer) observations have been selected, the elements of eqns. (3) are calculated using assumed analytic forms for the field correlations. The coefficient matrix is symmetric and positive definite. An iterative method--the method of conjugate gradients (Beckman, 1960)--is used to determine the solution. Experience has shown that convergence is customarily quite rapid. Rarely, an ill-conditioned matrix is encountered, which leads to slow convergence or divergence, and an unreliable solution. Such cases invariably arise because of a pair of observations located very close together. The difficulty is circumvented by dropping the one of the pair that has the lower correlation with the gridpoint, and repeating the solution process.

4. Filtering the correction field

One of the consequences of the decision to limit the number of observations affecting an update is that the stations selected tend to be those closest to the gridpoint to be updated. The result is a field of corrections which contain significant spatial "noise." Before adding the corrections to the guess, the noise is eliminated by use of a filter. A least-squares fit of the corrections by a series of spherical harmonics is performed, using triangular truncation and resolution of up to 24 modes. The reconstructed correction field therefore does not contain high wavenumber modes. It is then added to the predicted field, in the adjusted model coordinate, and the update is complete.

The filter is included in the system as an option. For the particular results shown in the following section, the filter was not used.

C. Initialization

As indicated previously, the updating of temperature and wind is done simultaneously, such that the corrections are related through the thermal wind. In practice, however, most of the updates prove to be univariate in data-dense areas. This is another consequence of the decision to limit the number of observations affecting an update. With only ten permissible observations, the selection procedure tends to select temperatures to update temperatures, and winds to update winds. A result of this is that the introduction of fresh data on a local basis invariably disturbs the balance between the mass and motion fields to some degree. In general, the larger the correction, the greater the resulting imbalance. Restoration of balance through the geostrophic adjustment process requires a period of time which depends in part on the characteristics of the prediction model and in part on the magnitude of the initial imbalance. If the adjustment interval is greater than the update interval, an accumulation of gravitational noise may result.

Accordingly, a dynamic initialization option is incorporated into the system after the update has been completed. The procedure consists of integrating forward and backward around the time of update using the Euler-backward (Matsuno, 1966) damping time integration method, much like

the procedure suggested by Nitta and Hovermale (1969). The duration of the initialization period is specified in advance. Irreversible physical processes, such as precipitation, are not permitted during the initialization.

D. Computational requirements

At the present time, the latitude-longitude grid mesh has a resolution of 5 degrees, and the vertical structure is represented by eight layers with a top at 50 mb. Updating is done each 6 hours, with available observations treated as synoptic over a ± 3-hour interval centered on the update time. A typical update requires approximately 12 minutes (CPU) to complete on the IBM 360/195.

III. Results of Initial Testing

For the first test of the assimilation system, interest centered on its general performance characteristics by comparison with those of the present NMC operational system. Beginning with the 12-hour NMC operational global forecast valid at 00 GMT 18 August 1975, the system was integrated through 00 GMT 20 August 1975, updating each 6 hours. The initialization procedure described previously was used at each update for the equivalent of 6 hours. In addition, a divergence-damping viscosity term (Dey, 1977) was used in the model stratosphere to control the growth of divergence, an unpleasant characteristic of the 8-layer version of the prediction model.

For comparison, a special cycle simulating the NMC operational system was conducted. The 5-degree, 8-layer prediction model was updated each

6 hours by the spectral objective analysis procedure developed by Flattery (1970). No initialization or divergence control was used during this special cycle. This integration will subsequently be referred to as the control system. Both began from the same initial state, but thereafter cycled independently. Both had access to the same data base; but the error-checking procedures are different for each system and, therefore, there is no guarantee that each system used exactly the same observations. In practice, the number each uses is very similar.

As a first indication of the performance of the assimialtion system, Figure 3 shows 300-mb height and isotach fields valid at 00 GMT 19 August 1975. This chart was produced by interpolating the updated fields of wind and temperature (and hydrostatically calculating the heights) from the model's vertical coordinates to standard isobaric levels. The control 300-mb height-isotach chart comparable to Figure 3 is shown in Figure 4. The first observation that may be made is that the two representations are very similar. Since both have access to the same data, this is to be expected. Nevertheless, differences may be found by closer inspection. Figures 5 and 6 show the difference field for height and wind speed, respectively. As a general rule, the differences in both are smallest in data-dense areas, and greatest in data-sparse areas. There are some exceptions, most notably over central Asia. In most instances, these are attributable to differences in the rejection criteria, or the treatment of

surface data, between the two systems. The fact that the control system treats heights directly, while the assimilation system calculates heights diagnostically from temperatures and surface pressure, no doubt also contributes to the difference.

A particularly interesting difference, and one that is synoptically significant, is the triplet of height differences in the north central Pacific. Close examination of Figure 3 reveals a short wavelength trough near 168E and a downstream minor ridge near 178E, both of which are supported by wind data from Kamchatka eastward to the dateline. These features are not apparent in the corresponding control field, and result in the difference pattern in Figure 5.

Another interesting difference occurs in the data-sparse area just off the west coast of North America. There, the assimilation system shows a wind maximum stronger by 10 m sec^{-1} than that in the control. There are only two observations--both are cloud-tracked winds of 50 kts at 34,000 feet--and neither supports the higher wind speeds shown by the assimilation system. A search for the origin of this discrepancy led to an examination of the previous history. Twenty-four hours earlier, both systems had indicated a large wind maximum in excess of 90 kts centered in the vicinity of Ocean Station Vessel 4YP (50N, 145W), which reported a wind speed of 125 kts. At the next update time, there were no observations in the area. Both systems moved the wind speed maximum to the southeast, but the control reduced its magnitude somewhat. This process continued at the next two

update times, so that by 00 GMT on 19 August the control system's wind maximum had been reduced to near 50 kts while the assimilated system had retained windspeeds near 90 kts. In the absence of data, it is difficult to determine which solution is more correct.

This difference serves to illustrate one of the two main design tenets of the assimilation system: to make no arbitrary or incidental changes to the model representation in the absence of data. The control system demonstrably reduced the windspeeds in this instance, most probably as a result of repeated filtering, through transformations between grid space and phase space, and also between isobaric and model coordinates. A part of the filtering involves the near complete removal of the divergent wind component.

Close perusal of Figure 6 suggests that, in general, the difference in wind speed is positive, meaning that the assimilation system exhibits higher wind speeds on the average. This is confirmed by Figure 7, the total kinetic energy in each system as a function of time. It is quite clear that the assimilation system shows higher kinetic energy. It is not clear that this is necessarily favorable.

In summary, the assimilation system appears to function reasonably well and compares favorably to the simulated operational system in areas where observations are dense. Differences do develop with time, mainly over data-sparse areas. The most noticeable difference is the higher kinetic energy level of the assimilation system.

IV. Future Plans

The assimilation system is being modified to use the 9-layer version of the prediction model. This version has demonstrably superior noise characteristics. Simultaneously, a major effort is being made to improve the observational error specifications in Table 1 and to upgrade the quality control procedures. It is anticipated that the horizontal resolution in the system will be increased to 2.5 degrees, at least in the prediction model, by late spring 1977. As these modifications are made, the performance of the assimilation system will be measured against an appropriate version of the control system.

As yet, the assimilation system is in a very early state of development. Much work remains before it can be considered a competitor of the present NMC operational system. Nevertheless, the results of these first experiments serve to encourage the effort.

Table 1

Observational Errors in Upper-Air Analysis

Type of Observation	Temp (^{o}C)	Wind ($m\ sec^{-1}$)	Spec. Hum.
"Bogus"	0.5	1.0	$.25\ [.002-3(1000-p_k)x10^{-6}]$
RAOB	1.0	$1+(1000-p_k)/1000$	$.50\ [.002-3(1000-p_k)x10^{-6}]$
Aircraft	1.0	2.0	$.50\ [.002-3(1000-p_k)x10^{-6}]$
VTPR SATOB	2.0	-	$1.0\ [.002-3(1000-p_k)x10^{-6}]$
900 mb Sat. Winds	-	3.0	-
200 mb Sat. Winds	-	7.5	-
Assumed Error of First Guess at Initial Time	2.0	5.0	$.002-3(1000-p_k)x\ 10^{-6}$

REFERENCES

Beckman, F. S., 1960: The solution of linear equations by the conjugate gradient method. Mathematical Methods for Digital Computers, Vol. 1, A. Ralston and H. S. Wilf, Eds., Wiley, 62-72.

Bergman, K. H., 1977: Multivariate objective analysis of temperature and wind fields using optimum interpolation. Manuscript in preparation, National Meteorological Center.

Cardone, V., 1969: Specification of the wind distribution in the marine boundary layer for wave forecasting. GSL Rpt. TR-69-1, Dept. of Meteorology and Oceanography, New York University.

Dey, C. H., 1977: Noise suppression in a primitive equation prediction model. Submitted to Monthly Weather Review.

Flattery, T. W., 1970: Spectral models for global analysis and forecasting. Proc. Sixth AWS Technical Exchange Conference, U.S. Naval Academy, Annapolos, Md., Air Weather Service Tech. Rpt. 242, 42-54.

Gandin, L. S., 1963: Objective analysis of meteorological fields. Gidrometeor. Izd., 242 pp. (Translated by Israel Program for Scientific Translations, Jerusalem, 1965).

Matsuno, T., 1966: Numerical integrations of the primitive equations by a simulated backward-difference method. J. Meteor. Soc., Japan, vol. 44, 76-84.

Nitta, T., and J. B. Hovermale, 1969: A technique of objective analysis and initialization for the primitive forecast equations. Mon. Wea. Rev., vol. 97, 652-658.

Rutherford, I. D., 1976: An operational three-dimensional multivariate statistical objective analysis scheme. Proc. J.O.C. Study Group Conference on Four-dimensional Data Assimilation, Paris, Nov. 17-21, 1975, 98-121.

Schlatter, T. W., G. W. Branstator, and L. G. Thiel, 1976: Testing a global multivariate statistical objective analysis scheme with observed data. Mon. Wea. Rev., vol. 104, 765-783.

Stackpole, J. D., L. W. Vanderman, and F. G. Shuman, 1974: The NMC 8-layer global primitive equation model on a latitude-longitude grid. GARP Publication Series, No. 14, WMO, Geneva, 79-93.

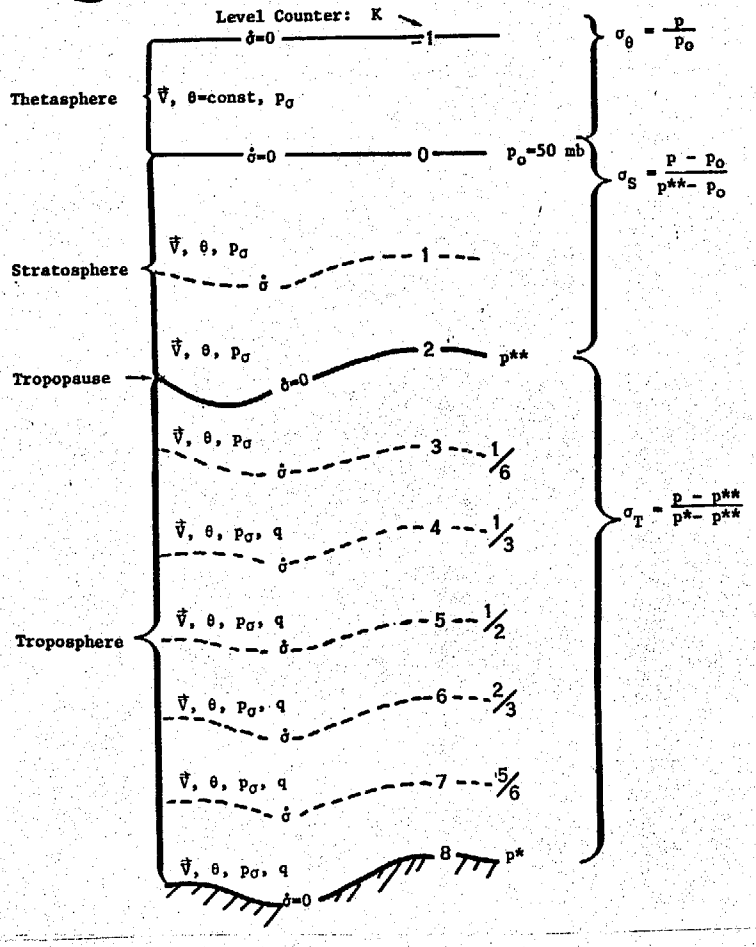

Figure 1. Vertical structure of the NMC 8-layer global prediction model.

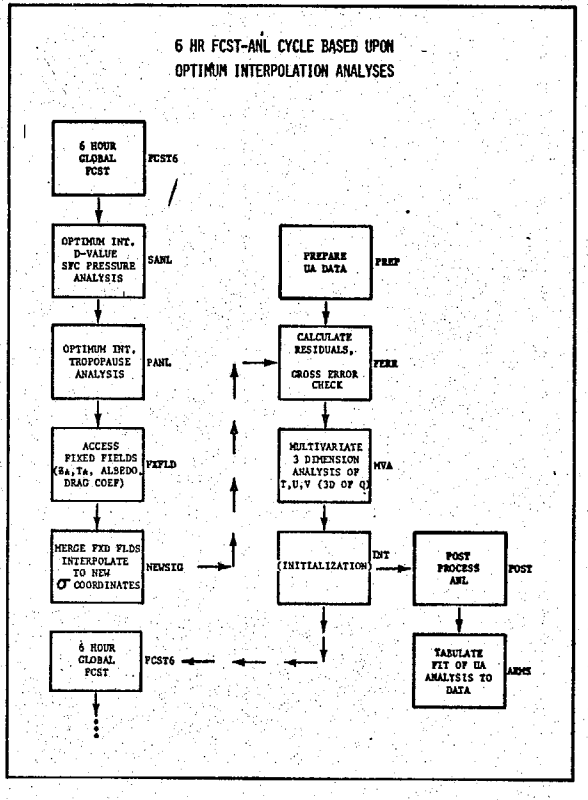

Figure 2. Schematic indicating the sequence of significant elements of each update.

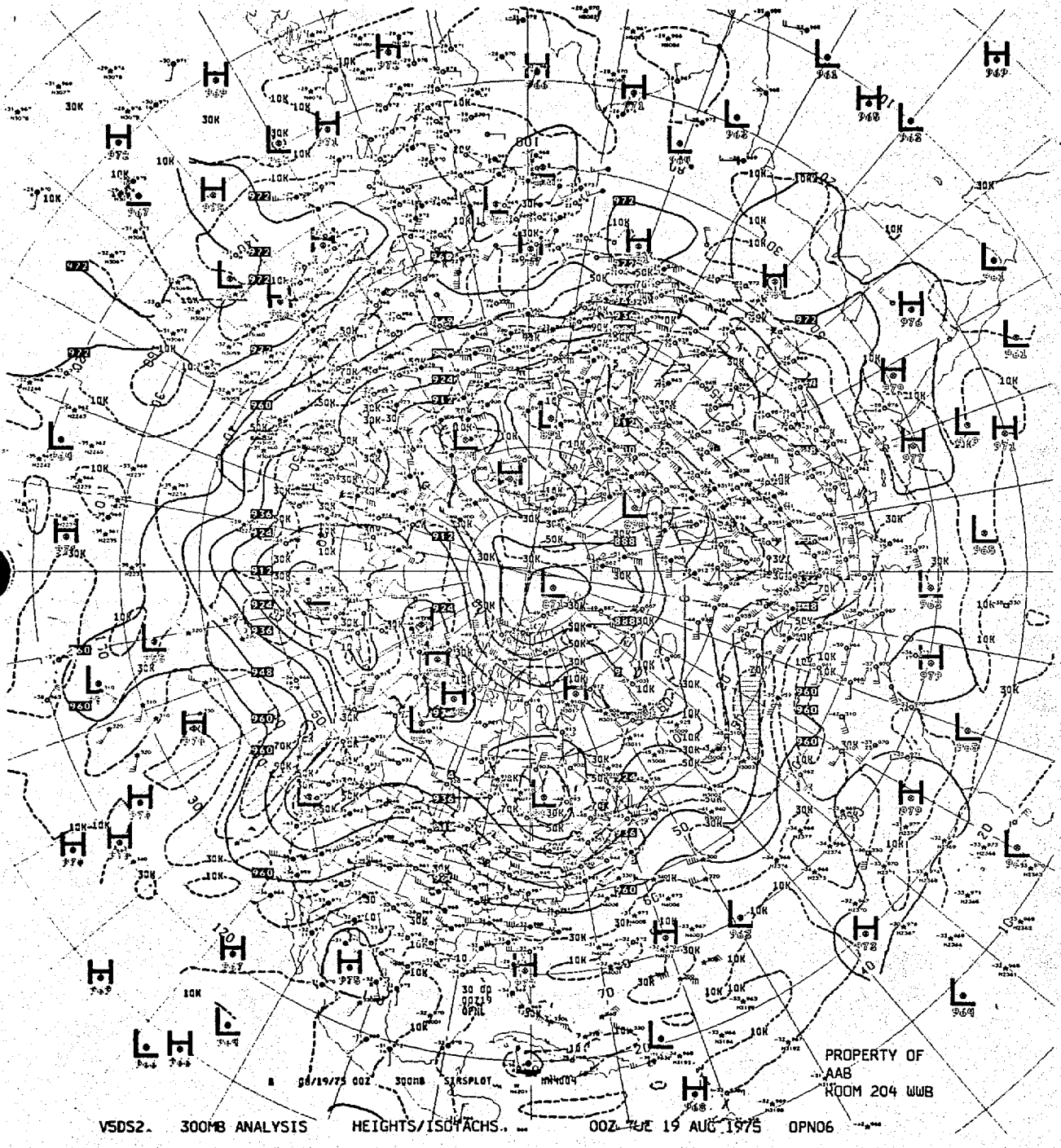

Figure 3. Heights and isotachs at 300 mb produced by vertical interpolation from the assimilation system's vertical coordinates together with plotted 300-mb data. The plotting model is as follows: circles represent radiosonde reports, squares represent aircraft reports, and stars represent both cloud-tracked wind vectors and observations deduced from satellite-borne radiometric measurements.

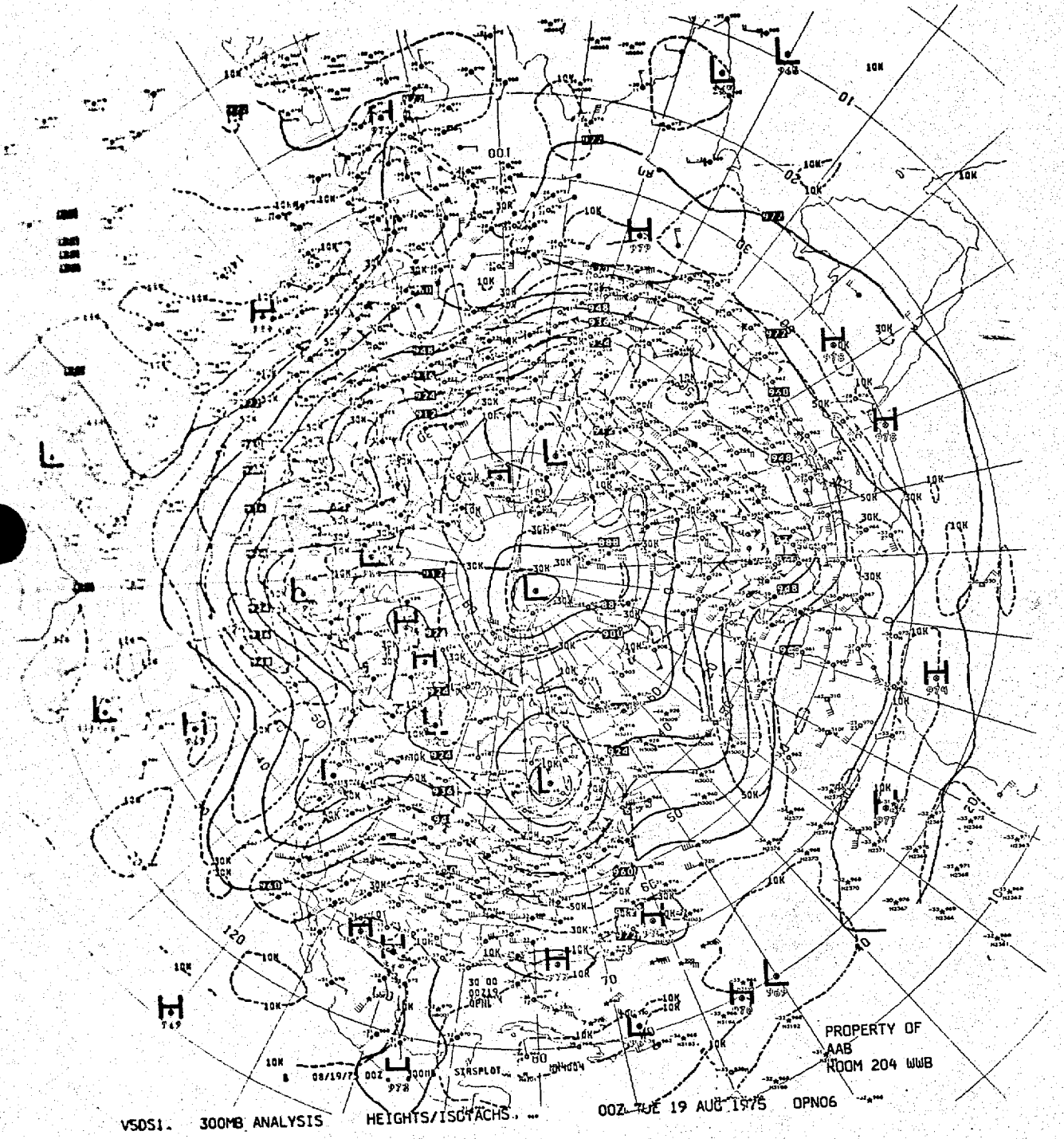

Figure 4. Same as Figure 3, but produced by the control system.

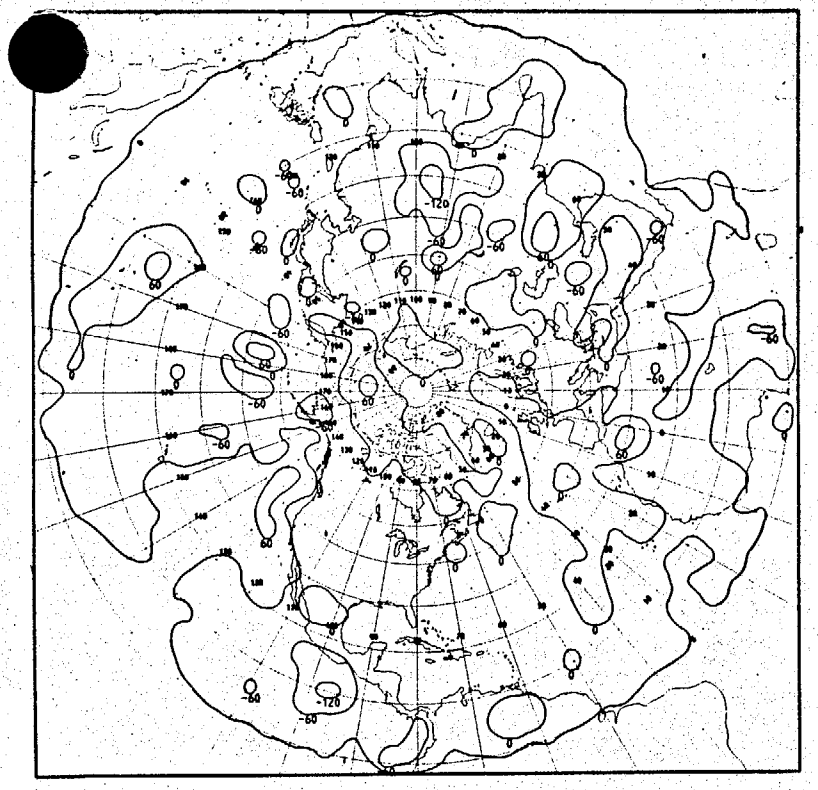

Figure 5. Difference (assimilation-control) of the height fields in Figs. 3 and 4. Contoured at 60m intervals.

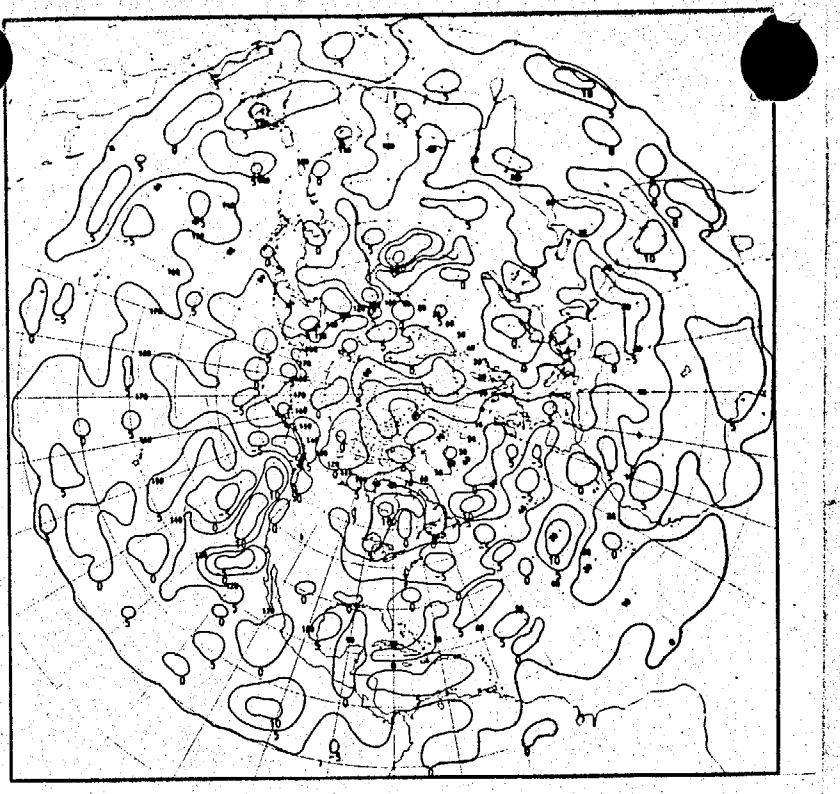

Figure 6. Difference (assimilation-control) of the wind-speed fields in Figs. 3 and 4. Contoured at 5 m sec^{-1} intervals.

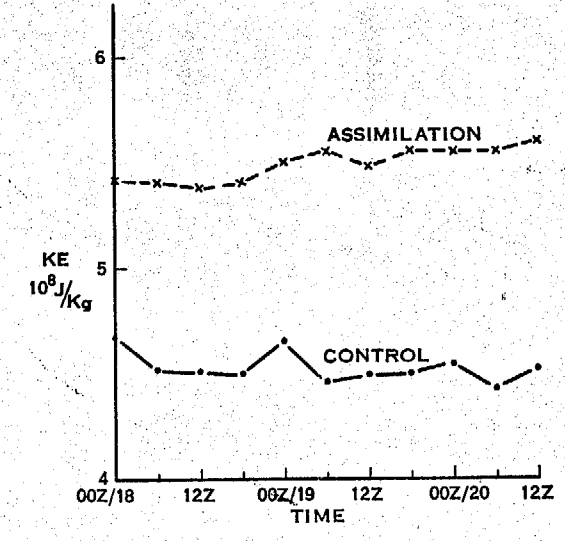

Figure 7. Total kinetic energy (joules/kilogram) as a function of time for the assimilation and the control integrations.

Table 1. Root-mean-square vector wind errors (kts), verifying against 26 western North American radiosonde stations. All three analyses started from the "poor" first-guess.

Level (mb)	"Poor" Guess	Operational Case 1	Strict Wind Law Case 2	Blended Case 3
850	11.8	13.7	15.5	13.9
500	22.2	16.1	14.4	15.8
300	33.2	24.6	21.6	23.9
100	8.6	8.2	8.7	8.1

Table 2. Root-mean-square vector wind errors (kts) using "good" first-guess and the same set of verification stations as used in Table 1.

Level	"Good" Guess	Operational Case 1	Strict Wind Law Case 2	Blended Case 3
850	11.7	12.8	14.3	12.9
500	12.2	12.6	12.8	12.5
300	18.2	17.6	18.7	17.6
100	8.9	10.2	12.1	10.3

Table 3. Root-mean-square height errors (m) using the same set of verification stations as in Tables 1 and 2.

	"Poor" Guess			"Good" Guess		
Level(mb)	Case 1	Case 2	Case 3	Case 1	Case 2	Case 3
850	9.2	9.3	9.3	8.8	8.9	8.8
500	11.1	11.2	11.5	10.1	10.1	10.3
300	21.6	21.6	21.9	21.4	21.4	21.6
100	16.4	16.4	16.3	17.6	17.6	17.7